water

MDPI

Article

The Simultaneous Analysis of Droplets' Impacts and Heat Transfer during Water Spray Cooling Using a Transparent Heater

Vladimir Serdyukov *, Nikolay Miskiv and Anton Surtaev

Laboratory of Low Temperature Thermophysics, Kutateladze Institute of Thermophysics SB RAS, Academician Lavrent'ev Avenue 1, 630090 Novosibirsk, Russia; nikerx@gmail.com (N.M.); surtaev@itp.nsc.ru (A.S.)

* Correspondence: vsserd@gmail.com

Abstract: This paper demonstrates the advantages and prospects of transparent design of the heating surface for the simultaneous study of the hydrodynamic and thermal characteristics of spray cooling. It was shown that the high-speed recording from the reverse side of such heater allows to identify individual droplets before their impact on the forming liquid film, which makes it possible to measure their sizes with high spatial resolution. In addition, such format enables one to estimate the number of droplets falling onto the impact surface and to study the features of the interface evolution during the droplets' impacts. In particular, the experiments showed various possible scenarios for this interaction, such as the formation of small-scale capillary waves during impacts of small droplets, as well as the appearance of "craters" and splashing crowns in the case of large ones. Moreover, the unsteady temperature field during spray cooling in regimes without boiling was investigated using high-speed infrared thermography. Based on the obtained data, the intensity of heat transfer during spray cooling for various liquid flow rates and heat fluxes was analyzed. It was shown that, for the studied regimes, the heat transfer coefficient weakly depends on the heat flux density and is primarily determined by the flow rate. In addition, the comparison of the processes of spray cooling and nucleate boiling was made, and an analogy was shown in the mechanisms that determine their intensity of heat transfer.

Keywords: spray cooling; transparent heater; high-speed video recording; infrared thermography

Citation: Serdyukov, V.; Miskiv, N.; Surtaev, A. The Simultaneous Analysis of Droplets' Impacts and Heat Transfer during Water Spray Cooling Using a Transparent Heater. *Water* **2021**, *13*, 2730. https://doi.org/10.3390/w13192730

Academic Editor: Maksim Pakhomov and Pavel Lobanov

Received: 29 July 2021
Accepted: 28 September 2021
Published: 2 October 2021

1. Introduction

Today, spray cooling is one of the most effective, reliable, and demanded modes of cooling and thermal stabilization of various heat-generating devices. Among its main advantages are the ability to remove high heat fluxes while ensuring a sufficiently uniform surface temperature, the ability to cool objects of complex (not flat) geometry and with a relatively large area even using a single nozzle, and a low liquid flow rate [1–4]. For these reasons, this process nowadays is used in different industrial cycles and technologies. In addition to traditional quenching in metallurgy, spray cooling is used in medical and aerospace technologies, as well as in fire safety systems. Moreover, application and optimization of jet and spray cooling systems are widely discussed today in relation to the development of high heat flux cooling solutions [5], e.g., heat exchangers for hydrogen storage, rocket nozzles, laser and microwave directed energy weapons, advanced radars, and so on. Finally, the relevance of the development of such systems for cooling high-performance microelectronic devices [6], computers and data centers [7], and high-power LEDs [8] should be noted. As the literature analysis shows, in the majority of applications with spray cooling, the main working fluid is water, first of all, because of its high heat capacity and enthalpy of vaporization, which makes it possible to remove sufficiently

high heat fluxes up to 900 W/cm^2 [9]. In addition, this coolant has a low cost and high environmental friendliness, and is simple and safe to use.

In this regard, many studies are devoted today to the processes during spray cooling, the description of which could be found in recent review papers [3,4,10]. At the same time, the analysis of these works shows that some issues related to the dynamics of liquid irrigation and heat transfer during spray cooling still remain open. First of all, this is because of the fact that spray cooling is an extremely difficult process for experimental study, and it is necessary to analyze a whole complex of its hydrodynamic and thermal characteristics. Often, it is possible to investigate in detail only one or several parameters of spray irrigation using a certain measuring technique. In particular, one of the most important parameters is the size and velocity of droplets in the gas-droplet flows. Today, these characteristics are measured using such methods as a side-view video recording, laser phase-Doppler particle analyzer, laser diffraction, interferometric particle imaging, and so on [11]. However, these methods do not allow to analyze the patterns and features of spray irrigation.

There are also many questions related to the heat transfer during spray cooling. In the overwhelming majority of experimental studies, measurements of thermal characteristics are carried out using thermocouples and local temperature sensors with low temporal and spatial resolutions. At the same time, as the results of a number of works show, the temperature field of a heater during spray cooling can be non-uniform depending on the irrigation mode [12]. General data do not allow to obtain information on the local unsteady characteristics of heat transfer and to assess their contribution to integral heat transfer. This hindered the understanding of the governing mechanisms of heat transfer, which is very important for the development of theoretical models to describe the process and engineering methods to calculate systems with jet or spray cooling. This indicates the need to introduce new methods with high spatial and temporal resolutions for the comprehensive study of the spray and jet irrigations' features.

As sprays and aerosols represent particle-laden flows [13,14], some questions related to the flow dynamics and features of droplets motion are also of interest. For example, the clustering and collision of droplets can affect how they will interact with an impact surface. In turn, this can have a significant influence on the local and, consequently, total heat transfer rate during spray cooling. Today, in the literature, numerous papers devoted to both the experimental and numerical investigations of the mentioned and other phenomena could be found. For example, the authors of [15,16] studied the relative motion of monodisperse high Stokes number particle pairs. The effect of gravity on the clustering and collision of bidisperse inertial particles was investigated in [17]. In [18], the relative dispersion of tracer particles was analyzed.

To study the processes of heat and mass transfer in various two-phase systems, the transparent design of a heating surface is actively used today. For example, such a design has been successfully applied by a number of researchers to analyze the characteristics of liquid boiling using high-speed video recording from the bottom side of a heating surface [19–23]. An analysis of the presented results shows that this makes it possible to study in detail the dynamics of vapor bubbles, to carry out a detailed statistical analysis of the bubbles departure diameters, the emission frequencies, and the nucleation site density in a wide range of heat loads. Moreover, this recording format allows to study the dynamics of the triple contact line at the bubble base under various conditions [24–26].

In addition to the visualization of two-phase systems' dynamics, the design of a transparent heating element also makes it possible to simultaneously study the surface unsteady temperature field using high-speed thermographic recording. For example, the authors of [27–31] used heaters based on a sapphire substrate with a deposited transparent indium-tin oxide film. As the result, both integral surface temperature and the features of local heat transfer in the vicinity of a triple contact line during nucleate boiling of various liquids were analyzed. In addition, such a recording was used to study the heat transfer during droplet impact on a liquid film. In particular, in [32], a water droplet impact

on a thin heated wafer, which is being cooled by a film flow generated from water jet impingement, was studied using IR recording. The authors showed that the drop impact breaks the steady-state cooling and causes a change in local temperature around the drop landing location.

The usage of a transparent heating surface also showed its perspectives for studying the interface evolution during the interaction of a single droplet and liquid film [33–36]. In particular, the authors of [33] showed various scenarios for drop impact on a film of water and a glycerol–water mixture. However, studies using such a promising design of the impact surface to investigate the characteristics of spray or multi-jet cooling today are still of a single nature. Here, only an early paper can be noted, for example, refs. [37–39] and others, in which the authors used transparent surfaces primarily to study integral irrigation patterns and identify the interaction between bubbles and impinging droplets. However, issues such as the sizes and number of droplets falling onto the surface were not considered. In addition, there are few works devoted to the study of the surface temperature distribution during spray cooling. It is obvious that carrying out experimental studies devoted to a detailed consideration of all key aspects of the mass and heat transfer will make it possible to obtain a large array of new experimental information. Such information will be useful for the creation of generalized dependencies describing the intensity of spray cooling.

The aim of the present study was the comprehensive investigation of the spray cooling features using a special design of the impact surface. Experimental data on the main hydrodynamic and thermal characteristics of spray irrigation were obtained using high-speed video visualization and thermography from the reverse side of a transparent heating element.

2. Materials and Methods

2.1. Experimental Setup and Transparent Heater Construction

The principal scheme of the experimental setup used to study the hydrodynamic and thermal parameters of spray cooling is presented in Figure 1. The setup consists of four basic sections: a circuit to supply gas-droplet multiphase flow, a spray nozzle, a transparent impact surface with a heating system, and high-speed video/infrared cameras.

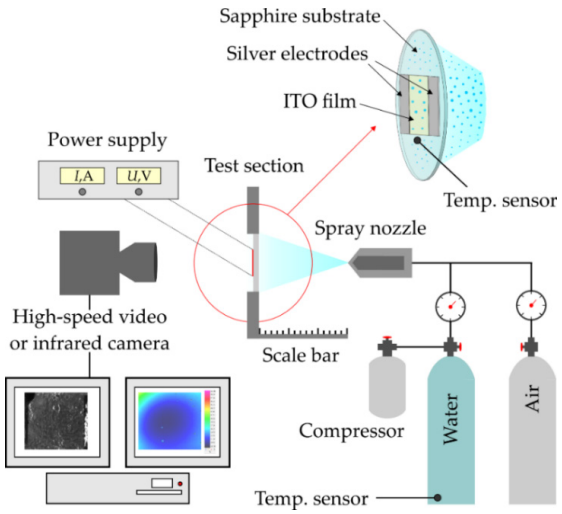

Figure 1. Schematic view of the experimental setup and the test section.

The key feature of the experimental setup is an optically transparent impact surface with a thin-film heater based on indium tin oxide (ITO), deposited onto a sapphire substrate by ion sputtering (ISP SB RAS). In this method, a commercially fabricated ITO target (Girmet Ltd., Moscow, Russia) was bombarded with argon ions. Such a technique allows one to fabricate smooth and uniform films with a given thickness. The main property of ITO is transparency in the visible range of wavelengths (380–750 nm) and opacity in the IR

range (3–5 μm), which makes it possible to simultaneously record the irrigation pattern using video recording and measure the surface temperature using IR thermography. A similar heater design was previously used in experiments on liquid boiling [25–27] and has shown its high prospect for the simultaneous study of the evolution of the liquid–vapor system and the temperature field of the heating surface. The thickness of the used sapphire substrate was 400 μm and the thickness of the ITO film heater was 1 μm. The area of direct heat release was 20 × 20 mm^2 and the spray irrigated the vertically oriented sapphire surface. The density of the supplied heat flux was measured according to the current passed through the heater and the potential difference between the silver current leads, also deposited by the ion sputtering technique along the edges of the ITO heater. At this stage of the study, the single-phase heat transfer during spray cooling without the development of boiling was studied, and the maximum heat flux density was 133 kW/m^2.

2.2. Spray Flow Parameters

The BKT-Engineering SS 4230 nozzle made of stainless steel and providing full cone spray was used in the experiments. The orifice diameter of the selected nozzle was 1.7 mm. Deionized MilliQ water was used as a working fluid and air was used as a working gas. The temperature of the working phases in all experiments was equal to room temperature (25 °C) and the relative humidity of the ambient air was 65%. The nozzle-to-surface distance was configured such that the spray impact area just inscribed the heating surface. Thus, to define the mean volumetric flux on a surface [40], the following expression can be used:

$$\overline{Q}'' = \frac{Q}{\pi L^2/4}, \quad (1)$$

where Q is the volumetric flow rate and L is the surface length.

The variation in the flow rate was ensured by maintaining the overpressure of the phases in the range from 1 to 3 bars at the nozzle inlets. In addition, the change in the parameters of spray irrigation was controlled by changing the position of the nozzle shut-off valve. In the experiments, three different spray irrigation regimes, so-called intermediate and dense spray [3] with either smooth or highly perturbed liquid film, as will be shown below, characterized by different irrigation patterns, were studied. In Figure 2, the measured values of the volumetric flow rate Q and the mean volumetric flux on a surface Q'' for the studied irrigation regimes are shown depending on the liquid overpressure. The minimum studied volumetric flow rate was 0.05 mL/s and the maximum was 1.7 mL/s.

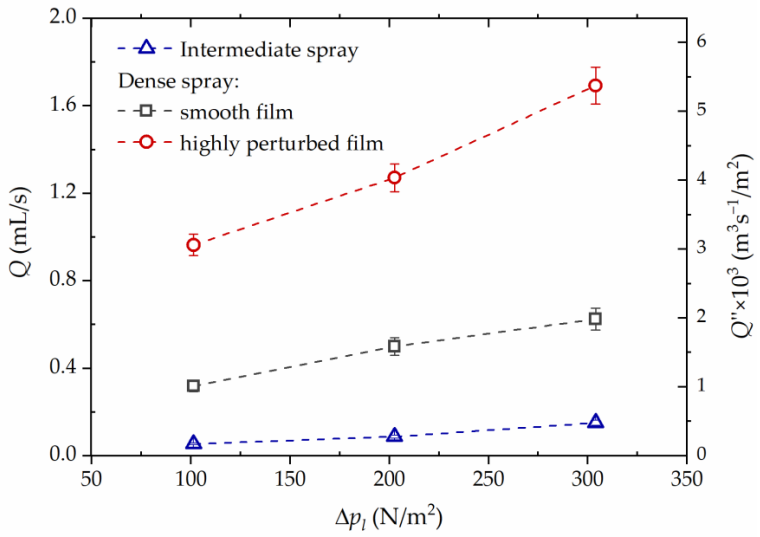

Figure 2. Liquid flow rates for the studied spray cooling regimes. The error bars are presented for the Q values.

As the analysis of the literature shows, the Stokes number (St) is also one of the key parameters of particle-laden flows, among which are spray flows. In particular, two types of situations can be observed for droplets suspended in gas flow: (a) if the St << 1, then the droplet will have ample time to respond to changes in gas flow velocity; (b) vice versa, for the case of St >> 1, the droplet has essentially no time to respond to the gas velocity changes and the its velocity will be little affected by the gas velocity change. The Stokes number is defined as the ratio of the particle momentum response time over a flow system time:

$$St = \frac{\tau_d}{\tau_f}. \quad (2)$$

For considered in the study system the Stokes number has the following form:

$$St = \frac{\rho_d d_d^2}{18\mu_a} \frac{V_f}{d_0}, \quad (3)$$

where ρ_d and d_d are the density and size of the droplets, V_f is the velocity of a spray flow, μ_a is the dynamic viscosity of the gas phase, and d_0 is the orifice diameter of a spray nozzle. The estimations show that, for the spray flow studied in the paper the value of St number (3) varies in the range of 50–1300, which identifies it as inertial flow. Here, the velocity of droplets was estimated using the high-speed video recording from the side of the spray flow.

2.3. High-Speed Video and Infrared Recordings

To study the spray irrigation patterns, a Phantom VEO 410L camera with a maximum frame rate of 100,000 fps and resolution of 30 μm per pixel was used. The analysis of the obtained video shows that the recording format from the reverse side of a heater allows to provide in one experiment an extensive dataset on the hydrodynamic characteristics of spray irrigation. Figure 3 demonstrates the advantages of using a transparent design of the heating surface and the high-speed visualization from its reverse side. As can be seen from the figure, it becomes possible to study the integral characteristics of irrigation; for example, to determine the area of wetted regions for low liquid flow rates, to estimate the characteristic number of liquid droplets falling onto the impact surface, to analyze the uniformity of irrigation, and so on. In addition, it is possible to identify single droplets before their interaction with either the impact surface or the forming liquid film. In turn, this allows to conduct a detailed statistical analysis of their size distribution. Finally, the used recording format allows to analyze the features of the interface evolution during the droplets' impacts on the liquid film forming on the heater.

To study the temperature field of the thin-film ITO heater, an FLIR Titanium HD 570 M high-speed infrared (IR) camera with a frame rate of 1000 fps and a resolution of 120 μm per pixel was used. Before the experiments, the calibration procedure for the IR camera was performed using a small-sized Honeywell temperature sensor located near the heater.

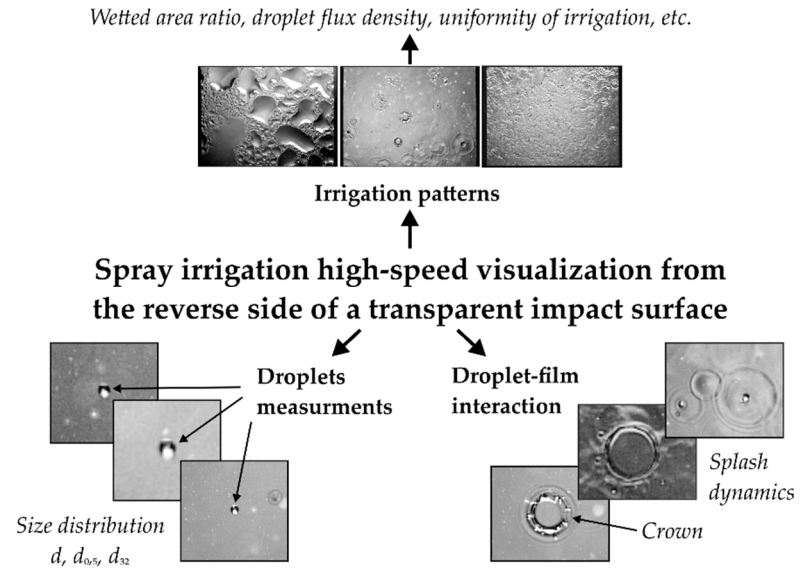

Figure 3. Prospects of using a transparent impact surface for studying the hydrodynamic parameters of spray irrigation.

2.4. Measurement Uncertainties

As the sizes of droplets were analyzed using high-speed video recording data, the uncertainty of such measurements is directly associated with the spatial resolution of the used camera. In turn, the errors of determining both average diameters and number (to analyze droplet flux density) of droplets for a given flow rate directly depend on the statistical error. To minimize it, the wide ensembles of droplets (up to 200–300 droplets) were analyzed in the study. The uncertainty of the time characteristics measurements is associated with the temporal resolution of the video camera, which was at least 0.05 ms. To study the features of the droplet–film interaction, the recording frequency was 100,000 fps, which provided the temporal resolution of 0.01 ms.

The maximum error in determining the value of the volumetric flow rate Q was 5%. The uncertainty of the heat flux density measurement includes an uncertainty associated with the current passed through the ITO heater and the corresponding voltage measurements. In total, their contribution is about 0.3%. However, to determine the real heat flux density supplied to the impact surface, it is necessary to evaluate the heat losses, which make the main contribution to the q value measurements' uncertainty. Based on the calculations made in Comsol Multiphysics, they were estimated to be less than 3% for the used heater design. Finally, according to the mentioned calibration procedure, the absolute error in measuring the surface temperature in the experiments did not exceed 1 °C.

3. Results

3.1. Irrigation Patterns

Using high-speed video recording from the reverse side of the impact surface, the irrigation patterns were studied for various liquid flow rates under adiabatic conditions (Figure 4). From the presented frames, it can be seen that, depending on the flow rate, there is a significantly different nature of the irrigation. In particular, for the so-called intermediate spray, the amount of liquid falling on the surface is not enough to form a continuous liquid film [3]. In this regime, the formation of the separate wetted areas up to 10 mm in size is observed on the impact surface. The coalescences of neighboring liquid areas into larger ones and their subsequent runoff from the surface under the action of gravitational forces are periodically observed. The second regime with a higher liquid flow rate is characterized by the continuous smooth liquid film formation, which is locally disturbed by falling droplets. In the presented frames, it is possible to clearly trace the interface evolution during the droplets' impacts on the film. For the next studied regime,

a liquid film with a significantly perturbed interface is observed on the impact surface, which is primarily caused by a significant increase in the droplet flux density.

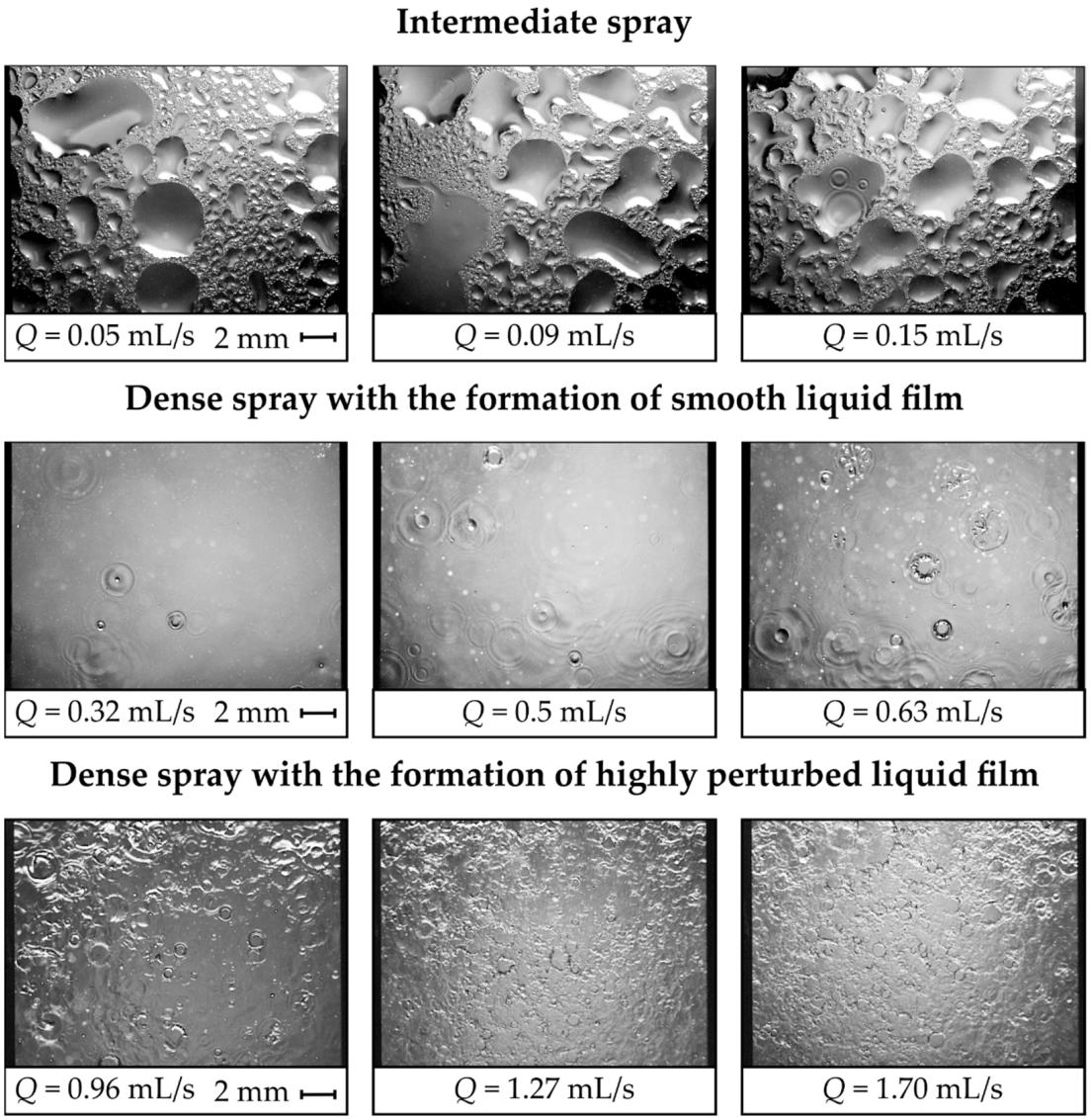

Figure 4. The various patterns during spray irrigation of the transparent impact surface investigated in the paper.

3.2. Droplet Sizes

As shown in Figure 3, owing to the high spatial and temporal resolutions of the used recording format and its focusing features, it is possible to identify and measure the sizes of droplets before their direct impact on the liquid film. This, in turn, makes it possible to obtain a detailed droplets' size distribution for various regimes. As an example, Figure 5a shows a histogram of the droplet diameter distribution for a liquid flow rate $Q = 0.5$ mL/s. It indicates that droplet sizes can vary over a wide range, from 40 to 170 μm for the presented case.

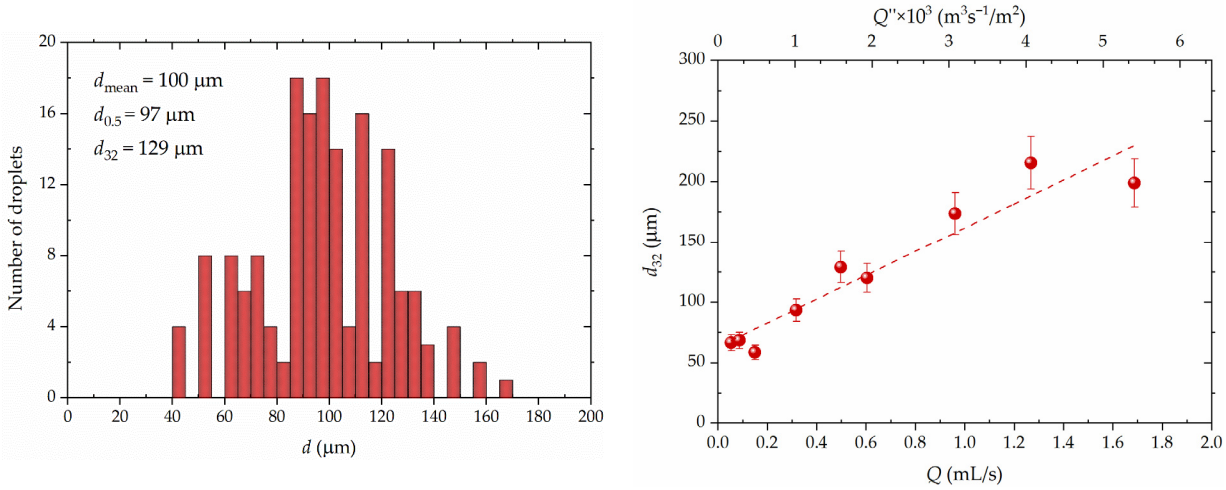

(**a**) (**b**)

Figure 5. (**a**) Droplet size distribution during spray irrigation (Q = 0.5 mL/s); (**b**) Sauter mean diameter dependence on the flow rate.

Using the obtained dataset, the values of the mass median diameter ($d_{0.5}$) and Sauter mean diameter (d_{32}) were determined, the last of which is defined as follows [41]:

$$d_{32} = \frac{\sum_i n_i d_i^3}{\sum_i n_i d_i^2}, \quad (4)$$

where n_i is the number of droplets with a diameter of d_i. Figure 5b demonstrates the dependence of the d_{32} value on the liquid flow rate. It can be seen that, with an increase in the liquid flow rate in the investigated range, the Sauter mean diameter increases and the obtained dependence d_{32} (Q) with an accuracy of ±25% is described by a linear function.

Certainly, the limit of the droplet diameter measurements in the considered visualization format is directly related to the spatial resolution of the video recording. With the use of special macro lenses, this parameter can be significantly improved; for example, as was done for visualizing individual bubbles during boiling on the surface of a microheater (resolution was 16 µm/pix) [42]. Therefore, in the authors' view, the recording format used is a promising method for measuring small-sized droplets of spray. It can be good alternative in some tasks to modern techniques such as laser diffraction, interferometric particle imaging, and others mentioned in the introduction.

3.3. Droplet Impact on Liquid Film

A particular interest of researchers today is associated with the evolution of the interfacial surface of a liquid film during the impact of individual droplets [43]. This interest is primarily owing the fact that the drop impact on the forming liquid film is one of the key mechanisms of spray cooling and plays an important role in the heat and mass transfer processes [44]. In particular, it can cause a sharp decrease in the impact surface temperature at the area of interaction. In this case, for a certain droplet size and velocity (We number), its impact leads to the formation of a so-called residual film [45]. In turn, this causes the enhanced convective heat transfer and enhanced synergy of velocity field and heat flow field inside the residual film [46]. It is interesting to note that this process is similar in mechanism to the sharp decrease in surface temperature during the nucleation during boiling. In this case, the evaporation of a thin layer of liquid formed at the base of the vapor bubble—the so-called microlayer [47]—leads to high local heat flux densities, exceeding up to 40 times the supplied heat flux [24,28,48].

The transparent design of the impact surface allows to study the scenarios of droplet–film interaction during spray cooling. Indeed, as can be seen from Figure 6, at a given

liquid flow rate (Q = 0.5 mL/s), various scenarios of the interface evolution are observed. Most of the small droplets (less than 100 μm) cause capillary wave disturbances on the film (Figure 6a). In this case, it seen that there is no noticeable change in the thickness or structure of the film. Moreover, the oscillations of the interface decay in a fairly short period of time.

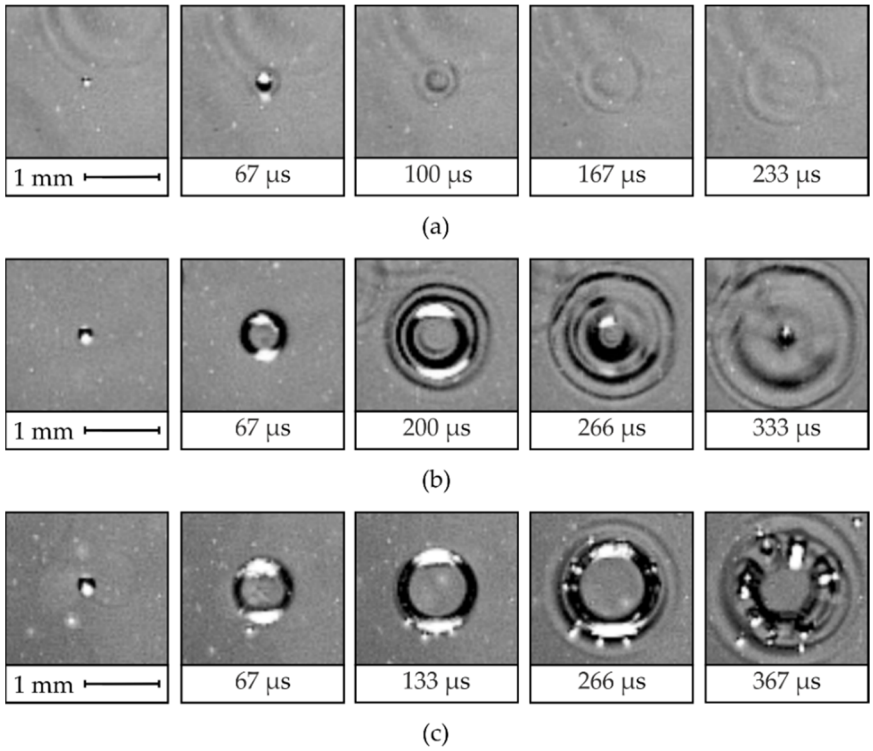

Figure 6. Various scenarios of the droplet impacts on the liquid film observed during spray cooling (Q = 0.5 mL/s): (**a**) small-scale wave disturbance caused by small droplets; (**b**) crater formation; (**c**) splashing crown.

For larger droplets (from 100 μm), the formation of large-scale and relatively long-term perturbations of the film is observed, accompanied by a noticeable change in the interface structure (Figure 6b). In particular, such droplets' impacts lead to the formation of craters with marked ejecta sheet, the depth of which can be comparable to the thickness of the liquid film. The diameter of such craters is up to 2 mm. In addition, large droplets can also cause splashing crowns (Figure 6c), both with and without the secondary droplets [43]. As the analysis of the mentioned literature shows, the last two described scenarios can lead to the formation of residual films. Therefore, droplets leading to such scenarios of the interface disturbance are of greatest interest when considering the mechanisms of heat transfer during spray cooling.

3.4. Droplet Flux Density

The droplet flux density is the number of droplets falling onto a unit of surface area per time unit:

$$\dot{N} = \frac{n}{A\tau}. \quad (5)$$

Similar to nucleation site density for nucleate boiling, the droplet flux density is an extremely important parameter for considering the intensity of mass and heat transfer during spray cooling. At the same time, given the impossibility of accurate measurement of the droplet flux density using the traditional visualization from the side of the impact surface, there are only few studies in the literature devoted to the analysis of this characteristic. This does not allow establishing the relationship of this parameter with the intensity of

heat transfer during spray cooling. In turn, the high-speed visualization from the reverse side of a transparent surface makes it possible to investigate this value even for high liquid flow rates. It is also important to note here that it becomes possible to analyze the number of droplets, whose impacts lead to the formation of the residual film described previously.

The determination of the $\dot{N}$ value was performed as follows. For each investigated flow rate, a region with a given area (A = 30 mm^2) was selected, and the number of droplets falling onto the surface within the boundaries of this area was counted for 500–800 ms. It is important to note that this technique makes it possible to count all droplets that come onto the surface, as even small droplets cause wave disturbances of the liquid film, which are clearly distinguishable in high-speed video frames (Figure 6a). The error of determining the droplet flux density in such way for small liquid flow rates directly depends on the statistical error. At high flow rates (more than 1.5 mL/s), counting the number of droplets becomes more difficult owing to the large number of local "events". In this case, the maximum measurement error of the $\dot{N}$ is up to 20%. However, it should be noted here that this value can be reduced, including through the use of automatic image processing algorithms, as well as neural networks, which will increase the sampling and improve the measurement accuracy.

Using the obtained video dataset, the droplet flux density was determined for various liquid flow rates. Figure 7 shows the comparison of the $\dot{N}$ values obtained for the central and edge regions of the surface for the liquid flow rates of Q = 0.32–0.63 mL/s. The figure demonstrates that, with an increase in the flow rate, the described parameter increases linearly. Meanwhile, the droplet flux density can vary significantly depending on the impact surface region selected for the analysis. In particular, for these flow rates, the number of droplets that come to the central region of the impact surface is on average 15% higher than those that come to the edge regions. Obviously, such unevenness is associated with the characteristics of the nozzle used. As will be shown below, this factor can significantly affect the distribution of the temperature field under the conditions of single-phase heat transfer. Thus, in addition to new experimental information about the droplet flux density, the visualization format considered in the study also allows to analyze the uniformity of spray irrigation, which is an extremely important aspect when choosing a nozzle.

3.5. Heat Transfer Rate

The use of high-speed infrared thermography made it possible to analyze the temperature field of the impact surface and to determine the intensity of heat transfer in various modes of spray cooling. For example, in Figure 8, the time-averaged IR thermography frame and the corresponding temperature distribution of the heating surface for a liquid flow rate Q = 1.7 mL/s and heat flux density q = 45 kW/m^2 are presented. The obtained temperature distribution indicates that there is a difference in temperature values at the center and at the periphery of the heating area. However, this difference for the presented case is no more than 3 °C, but it can increase with an increase in the heat flux density. This fact, in our opinion, is primarily owing to the non-uniform distribution of the droplet flux density over the surface, as demonstrated earlier (Figure 7).

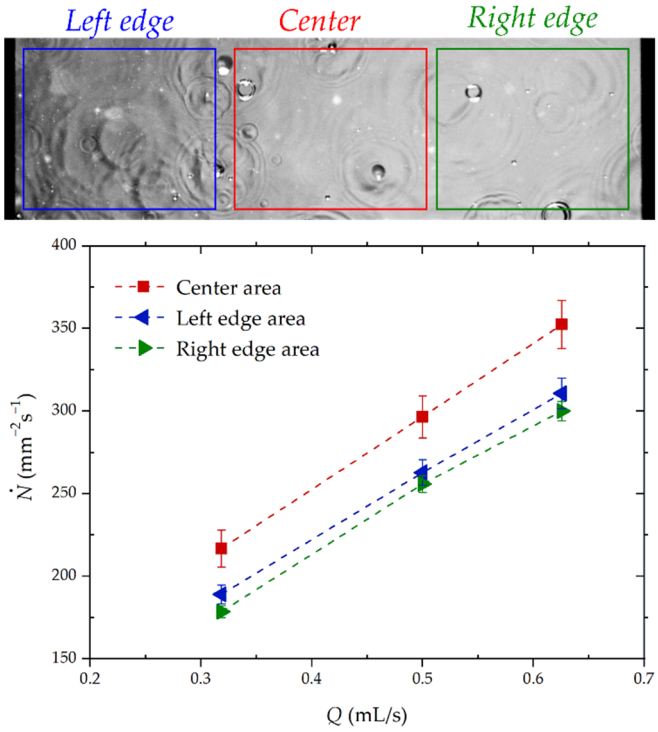

Figure 7. The dependence of the droplet flux density on the liquid flow rate for various impact surface areas.

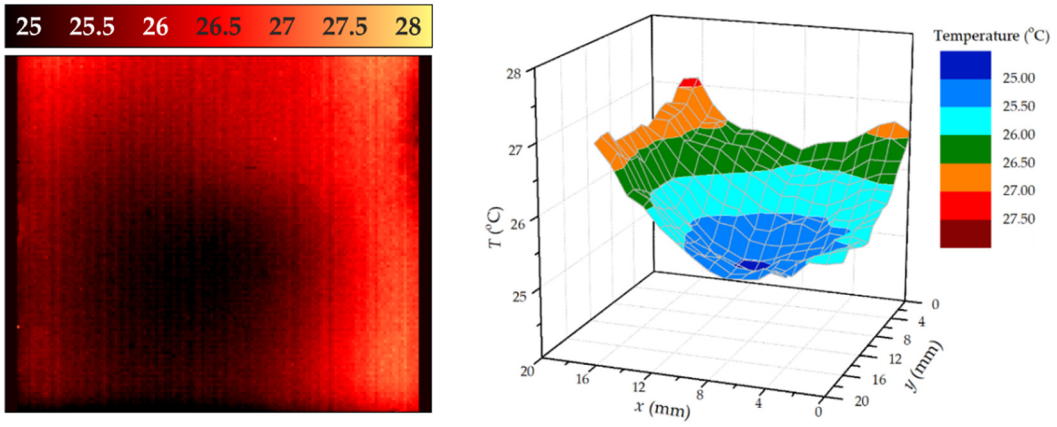

(**a**) (**b**)

Figure 8. (**a**) The time-averaged IR thermography frame and (**b**) corresponding temperature distribution of the heating during spray cooling (Q = 1.7 mL/s, q = 45 kW/m^2).

With the use of the obtained dataset on the surface temperature, the values of the heat transfer coefficient (HTC) for spray cooling were obtained:

$$\mathrm{HTC} = \frac{q}{\overline{T}_s - T_0}, \tag{6}$$

where $\overline{T}_s$ is the surface temperature averaged over time (10 s) and area and T_0 is the initial liquid temperature. Figure 9a shows the dependences of the HTC value on the heat flux density at various liquid flow rates. It seen that the intensity of single-phase heat transfer during spray cooling weakly depends on the heat flux in the studied range. At the same

time, an increase in the flow rate leads to a noticeable increase in the intensity of heat transfer (Figure 9b).

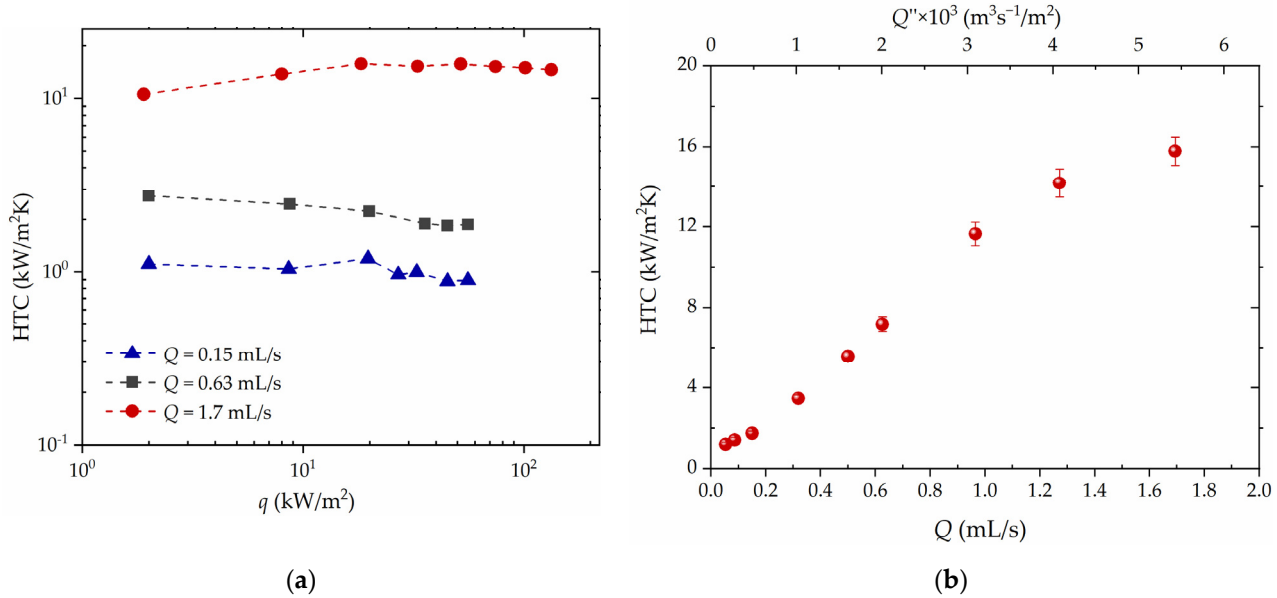

Figure 9. The dependence of the heat transfer coefficient during spray cooling on (**a**) heat flux density and (**b**) liquid flow rate.

At the next stage, the data on the intensity of single-phase heat transfer were compared with the existing correlations (Figure 10). For analysis, the models of Mudawar, Valentine [49], and Rybicki and Mudawar [50] were selected, which have the corresponding forms:

$$\mathrm{Nu} = 2.512\mathrm{Re}_s^{0.76}\mathrm{Pr}_f^{0.56}, \quad (7)$$

$$\mathrm{Nu} = 4.70\mathrm{Re}_s^{0.61}\mathrm{Pr}_f^{0.32}. \quad (8)$$

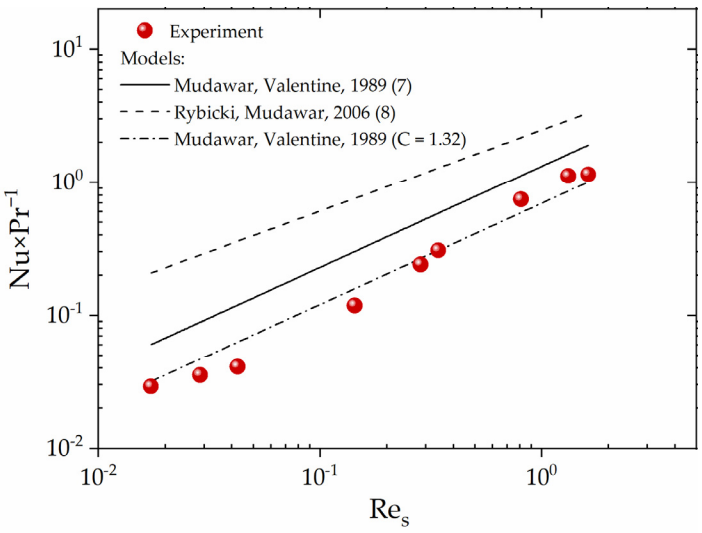

Figure 10. The comparison of the obtained data on the heat transfer intensity during spray cooling with the existing correlations (q = 45 kW/m^2).

In these models, mean volumetric flux on a surface (Q'') and Sauter mean diameter (d_{32}) are used as characteristic scales of velocity and length, respectively:

$$\mathrm{Nu} = \frac{\mathrm{HTC} \cdot d_{32}}{k_f}, \tag{9a}$$

$$\mathrm{Re}_s = \frac{\rho_f Q'' \cdot d_{32}}{\mu_f}, \tag{9b}$$

$$\mathrm{Pr}_f = \frac{C_{pf}\mu_f}{k_f}. \tag{9c}$$

A comparison with the presented models shows that they both demonstrate overestimated values in comparison with the obtained experimental data. Meanwhile, the character of the obtained dependence is close to the correlation [49] and the experimental data can be described within its framework when the numerical constant in expression (7) changes by 1.32.

It is interesting to note that the presented dependences (7) and (8) are close in their form to the criterion dependences used to describe heat transfer during nucleate pool boiling (without taking into account the effect of the properties of heat exchange surface) [51]. In particular, in [52], based on the large dataset generalization, the following dependence was obtained:

$$\mathrm{Nu}_* \sim \mathrm{Re}_*^{0.8}\mathrm{Pr}_f^{1/3}. \tag{10}$$

As can be seen from the comparison, the general view and the exponents at the similar numbers of expression (10) are close to expressions (7) and (8). In addition, as the characteristic dynamic scales of nucleate boiling, the capillary constant and the evaporation rate are used in (10). These parameters are similar to those used for spray cooling description (Figure 9a,b). Moreover, obtained in Figure 9b, the character of the HTC(Q) dependence during spray cooling,

$$\mathrm{HTC} \sim Q^{0.78}, \tag{11}$$

is close to the expressions used to describe heat transfer during nucleate boiling [51]:

$$\mathrm{HTC} \sim q^{0.6-0.8}. \tag{12}$$

Such similarity in the description of these two processes argues in favour of the hypothesis that the physical mechanisms of spray cooling and nucleate boiling are generally similar. In particular, the main contribution to heat transfer during spray cooling, like bubble formation for boiling, is provided by the droplet impact on the liquid film. Some difference in the exponents in the used expressions can be caused by the fact that, during spray irrigation, not all droplets impacting the film have a significant contribution to heat transfer. In particular, as noted earlier, only droplets with a sufficient Weber number form residual film and crown splashing, which lead to a noticeable change in the temperature field of the surface.

4. Conclusions

Using a transparent design of the heating surface and high-speed video and thermographic recordings, a comprehensive study of the hydrodynamic and thermal characteristics of spray cooling was performed with varying liquid flow rate and heat fluxes in a single-phase heat transfer regime. As a result, the following results were obtained:

- The study of the droplet size distribution was carried out and the dependence of the Sauter diameter on the liquid flow rate for the studied irrigation modes was obtained.
- The droplet flux density for various flow rates was studied. It has been shown that this parameter can differ significantly depending on the impact surface region. This

makes it possible to assess the degree of irrigation irregularity even in the case of a full cone spray.
- Various possible scenarios of interaction between droplets and a liquid film forming on the surface were shown, such as the formation of small-scale capillary waves for small droplets, as well as the appearance of craters and splashing crown in the case of large ones.
- Based on the data of high-speed infrared recording, the intensity of heat transfer during spray cooling for various heat flux densities and the liquid flow rates was analyzed. It was shown that, for the studied regimes, the value of the heat transfer coefficient is weakly dependent on the heat flux and is determined primarily by the flow rate.
- Comparison of the obtained experimental data on the intensity of single-phase heat transfer during spray cooling with existing models was performed. It was shown that data can be described within the model of [49] with a modified numerical coefficient. In addition, based on a comparative analysis of existing approaches, an analogy in the mechanisms that determine the intensity of heat transfer during spray cooling and nucleate boiling was shown.

Thus, the performed experimental study shows high prospects of using a transparent design of the heating surface to analyze the main characteristics of spray cooling. In particular, video recording from the reverse side of a transparent impact surface can serve as a good alternative to existing techniques, for example, laser diffraction, interferometric particle imaging, and so on. The authors hope that the information presented in this paper will be useful for further research in this area.

Author Contributions: Conceptualization, A.S. and V.S.; methodology, A.S., V.S. and N.M.; software, N.M.; validation, V.S.; formal analysis, N.M. and V.S.; investigation, V.S. and A.S.; resources, A.S.; data curation, N.M. and V.S.; writing—original draft preparation, V.S.; writing—review and editing, A.S. and V.S.; visualization, N.M. and V.S.; supervision, V.S. and A.S.; project administration, V.S.; funding acquisition, V.S. All authors have read and agreed to the published version of the manuscript.

Funding: The investigation was supported by the Ministry of Science and Higher Education of the Russian Federation (mega-grant No. 075-15-2021-575). The experimental setup was designed and built within the framework of the state contract with IT SB RAS (No. 121031800216-1).

Institutional Review Board Statement: Not applicable.

Informed Consent Statement: Not applicable.

Data Availability Statement: Not applicable.

Conflicts of Interest: The authors declare no conflict of interest.

References

1. Kim, J. Spray cooling heat transfer: The state of the art. *Int. J. Heat Fluid Flow.* **2007**, *28*, 753–767. [CrossRef]
2. Silk, E.A.; Golliher, E.L.; Selvam, R.P. Spray cooling heat transfer: Technology overview and assessment of future challenges for micro-gravity application. *Energy Conv. Mngt.* **2008**, *49*, 453–468. [CrossRef]
3. Liang, G.; Mudawar, I. Review of spray cooling—Part 1: Single-phase and nucleate boiling regimes, and critical heat flux. *Int. J. Heat Mass Transf.* **2017**, *115*, 1174–1205. [CrossRef]
4. Liang, G.; Mudawar, I. Review of spray cooling–Part 2: High temperature boiling regimes and quenching applications. *Int. J. Heat Mass Transf.* **2017**, *115*, 1206–1222. [CrossRef]
5. Mudawar, I. Recent advances in high-flux, two-phase thermal management. *J. Therm. Sci. Eng. Appl.* **2013**, *5*, 021012. [CrossRef]
6. Fabbri, M.; Jiang, S.; Dhir, V.K. A comparative study of cooling of high power density electronics using sprays and microjets. *J. Heat Transf.* **2005**, *127*, 38–48. [CrossRef]
7. Shedd, T.A. Next generation spray cooling: High heat flux management in compact spaces. *Heat Transf. Eng.* **2007**, *28*, 87–92. [CrossRef]
8. Khandekar, S.; Sahu, G.; Muralidhar, K.; Gatapova, E.Y.; Kabov, O.A.; Hu, R.; Luo, X.; Zhao, L. Cooling of high-power LEDs by liquid sprays: Challenges and prospects. *Appl. Therm. Eng.* **2021**, *184*, 115640. [CrossRef]
9. Yang, J.; Chow, L.C.; Pais, M.R. Nucleate Boiling Heat Transfer in Spray Cooling. *J. Heat Transf.* **1996**, *118*, 668–671. [CrossRef]

10. Xu, R.N.; Wang, G.; Jiang, P. Spray Cooling on Enhanced Surfaces: A Review of the Progress and Mechanisms. *J. Electron. Packag.* **2021**, *144*, 010802. [CrossRef]
11. Sijs, R.; Kooij, S.; Holterman, H.J.; Van De Zande, J.; Bonn, D. Drop size measurement techniques for sprays: Comparison of image analysis, phase Doppler particle analysis, and laser diffraction. *AIP Adv.* **2021**, *11*, 015315. [CrossRef]
12. Zhao, X.; Yin, Z.; Zhang, B.; Yang, Z. Experimental investigation of surface temperature non-uniformity in spray cooling. *Int. J. Heat Mass Transf.* **2020**, *146*, 118819. [CrossRef]
13. Salazar, J.P.; Collins, L.R. Two-particle dispersion in isotropic turbulent flows. *Annu. Rev. Fluid Mech.* **2009**, *41*, 405–432. [CrossRef]
14. Balachandar, S.; Eaton, J.K. Turbulent dispersed multiphase flow. *Annu. Rev. Fluid Mech.* **2010**, *42*, 111–133. [CrossRef]
15. Rani, S.L.; Dhariwal, R.; Koch, D.L. A stochastic model for the relative motion of high Stokes number particles in isotropic turbulence. *J. Fluid Mech.* **2014**, *756*, 870–902. [CrossRef]
16. Dhariwal, R.; Rani, S.L.; Koch, D.L. Stochastic theory and direct numerical simulations of the relative motion of high-inertia particle pairs in isotropic turbulence. *J. Fluid Mech.* **2017**, *813*, 205–249. [CrossRef]
17. Dhariwal, R.; Bragg, A.D. Small-scale dynamics of settling, bidisperse particles in turbulence. *J. Fluid Mech.* **2018**, *839*, 594–620. [CrossRef]
18. Ouellette, N.T.; Xu, H.; Bourgoin, M.; Bodenschatz, E. An experimental study of turbulent relative dispersion models. *New J. Phys.* **2006**, *8*, 109. [CrossRef]
19. Ohta, H. Experiments on microgravity boiling heat transfer by using transparent heaters. *Nucl. Eng. Design* **1997**, *175*, 167–180. [CrossRef]
20. Diao, Y.H.; Zhao, Y.H.; Wang, Q.L. Photographic study of bubble dynamics for pool boiling of refrigerant R11. *Heat Mass Transf.* **2007**, *43*, 935–947. [CrossRef]
21. Garrabos, Y.; Lecoutre, C.; Beysens, D.; Nikolayev, V.; Barde, S.; Pont, G.; Zappoli, B. Transparent heater for study of the boiling crisis near the vapor–liquid critical point. *Acta Astronaut.* **2010**, *66*, 760–768. [CrossRef]
22. Kaiho, K.; Okawa, T.; Enoki, K. Measurement of the maximum bubble size distribution in water subcooled flow boiling at low pressure. *Int. J. Heat Mass Transf.* **2017**, *108*, 2365–2380. [CrossRef]
23. Serdyukov, V.; Malakhov, I.; Surtaev, A. High-speed visualization and image processing of sub-atmospheric water boiling on a transparent heater. *J. Vis.* **2020**, *23*, 873–884. [CrossRef]
24. Jung, S.; Kim, H. An experimental method to simultaneously measure the dynamics and heat transfer associated with a single bubble during nucleate boiling on a horizontal surface. *Int. J. Heat Mass Transf.* **2004**, *73*, 365–375. [CrossRef]
25. Surtaev, A.; Serdyukov, V.; Zhou, J. Pavlenko, A.; Tumanov, V. An experimental study of vapor bubbles dynamics at water and ethanol pool boiling at low and high heat fluxes. *Int. J. Heat Mass Transf.* **2018**, *126*, 297–311. [CrossRef]
26. Surtaev, A.; Serdyukov, V.; Malakhov, I. Effect of subatmospheric pressures on heat transfer, vapor bubbles and dry spots evolution during water boiling. *Exp. Therm. Fluid Sci.* **2020**, *112*, 109974. [CrossRef]
27. Gerardi, C.; Buongiorno, J.; Hu, L.W.; McKrell, T. Study of bubble growth in water pool boiling through synchronized, infrared thermometry and high-speed video. *Int. J. Heat Mass Transf.* **2010**, *53*, 4185–4192. [CrossRef]
28. Serdyukov, V.S.; Surtaev, A.S.; Pavlenko, A.N.; Chernyavskiy, A.N. Study on local heat transfer in the vicinity of the contact line under vapor bubbles at pool boiling. *High. Temp.* **2018**, *56*, 546–552. [CrossRef]
29. Ravichandran, M.; Bucci, M. Online, quasi-real-time analysis of high-resolution, infrared, boiling heat transfer investigations using artificial neural networks. *Appl. Therm. Eng.* **2019**, *163*, 114357. [CrossRef]
30. Voulgaropoulos, V.; Aguiar, G.M.; Bucci, M.; Markides, C.N. Simultaneous Laser-and Infrared-Based Measurements of the Life Cycle of a Vapour Bubble During Pool Boiling. In *Advances in Heat Transfer and Thermal Engineering*; Wen, C., Yan, Y., Eds.; Springer: Singapore, 2021; pp. 169–173. [CrossRef]
31. Tanaka, T.; Miyazaki, K.; Yabuki, T. Observation of heat transfer mechanisms in saturated pool boiling of water by high-speed infrared thermometry. *Int. J. Heat Mass Transf.* **2021**, *170*, 121006. [CrossRef]
32. Gao, X.; Kong, L.; Li, R.; Han, J. Heat transfer of single drop impact on a film flow cooling a hot surface. *Int. J. Heat Mass Transf.* **2017**, *108*, 1068–1077. [CrossRef]
33. Gao, X.; Li, R. Impact of a single drop on a flowing liquid film. *Phys. Rev. E* **2015**, *92*, 053005. [CrossRef]
34. Josserand, C.; Thoroddsen, S.T. Drop impact on a solid surface. *Annu. Rev. Fluid Mech.* **2016**, *48*, 365–391. [CrossRef]
35. Kant, P.; Müller-Groeling, H.; Lohse, D. Pattern formation during the impact of a partially frozen binary droplet on a cold surface. *Phys. Rev. Lett.* **2020**, *125*, 184501. [CrossRef] [PubMed]
36. Ersoy, N.E.; Eslamian, M. Phenomenological study and comparison of droplet impact dynamics on a dry surface, thin liquid film, liquid film and shallow pool. *Exp. Therm. Fluid Sci.* **2020**, *112*, 109977. [CrossRef]
37. Yoshida, K.I.; Abe, Y.; Oka, T.; Mori, Y.H.; Nagashima, A. Spray cooling under reduced gravity condition. *J. Heat Transf.* **2001**, *123*, 309–318. [CrossRef]
38. Rini, D.P.; Chen, R.H.; Chow, L.C. Bubble behavior and nucleate boiling heat transfer in saturated FC-72 spray cooling. *J. Heat Transf.* **2002**, *124*, 63–72. [CrossRef]
39. Griffin, A.R.; Vijayakumar, A.; Chen, R.H.; Sundaram, K.B.; Chow, L.C. Development of a transparent heater to measure surface temperature fluctuations under spray cooling conditions. *J. Heat Transf.* **2008**, *130*, 114501. [CrossRef]
40. Mudawar, I.; Estes, K.A. Optimizing and Predicting CHF in Spray Cooling of a Square Surface. *J. Heat Transf.* **1996**, *118*, 672–679. [CrossRef]

41. Mugele, R.A.; Evans, H.D. Droplet size distribution in sprays. *Industr. Eng. Chem.* **1951**, *43*, 1317–1324. [CrossRef]
42. Surtaev, A.; Serdyukov, V.; Malakhov, I.; Safarov, A. Nucleation and bubble evolution in subcooled liquid under pulse heating. *Int. J. Heat Mass Transf.* **2021**, *169*, 120911. [CrossRef]
43. Liang, G.; Mudawar, I. Review of mass and momentum interactions during drop impact on a liquid film. *Int. J. Heat Mass Transf.* **2016**, *101*, 577–599. [CrossRef]
44. Breitenbach, J.; Roisman, I.V.; Tropea, C. From drop impact physics to spray cooling models: A critical review. *Exp. Fluids* **2018**, *59*, 1–21. [CrossRef]
45. Berberović, E.; van Hinsberg, N.P.; Jakirlić, S.; Roisman, I.V.; Tropea, C. Drop impact onto a liquid layer of finite thickness: Dynamics of the cavity evolution. *Phys. Rev. E* **2009**, *79*, 036306. [CrossRef]
46. Liang, G.; Zhang, T.; Chen, L.; Chen, Y.; Shen, S. Single-phase heat transfer of multi-droplet impact on liquid film. *Int. J. Heat Mass Transf.* **2019**, *132*, 288–292. [CrossRef]
47. Cooper, M.G.; Lloyd, A.J.P. The microlayer in nucleate pool boiling. *Int. J. Heat Mass Transf.* **1969**, *12*, 895–913. [CrossRef]
48. Golobic, I.; Petkovsek, J.; Baselj, M.; Papez, A.; Kenning, D.B.R. Experimental determination of transient wall temperature distributions close to growing vapor bubbles. *Heat Mass Transf.* **2009**, *45*, 857–866. [CrossRef]
49. Mudawar, I.; Valentine, W.S. Determination of the local quench curve for spray-cooled metallic surfaces. *J. Heat Treat.* **1989**, *7*, 107–121. [CrossRef]
50. Rybicki, J.R.; Mudawar, I. Single-phase and two-phase cooling characteristics of upward-facing and downward-facing sprays. *Int. J. Heat Mass Transf.* **2006**, *49*, 5–16. [CrossRef]
51. Thome, J.R.; Kim, J. *Encyclopedia of Two-Phase Heat Transfer and Flow II: Special Topics and Applications*; World Scientific Publishing Co. Pte. Ltd.: Singapore, 2015; pp. 62–79. [CrossRef]
52. Gogonin, I.I. The dependence of boiling heat transfer on the properties and geometric parameters of heat-transfer wall. *High Temp.* **2006**, *44*, 913–921. [CrossRef]